Synthesis of a novel monomer “DDTU-IDI” for the development of low-shrinkage dental resin composites

DOI:
10.1016/j.dental.2024.02.007

Document Version
Accepted author manuscript

Synthesis of a novel monomer "DDTU-IDI" for the development of low-shrinkage dental resin composites

Zixuan Zhou [a,b,1], Aihua Li [c,1], Ke Sun [a,b], Di Guo [a,b], Tingting Li [a,b], Jun Lu[a], Bruna S.H. Tonin [d], Zhou Ye[e], David C. Watts [f], Ting Wang[g,*], Jing Fu [a,b,*]

[a] *Department of Prosthodontics, The Affiliated Hospital of Qingdao University, Qingdao 266003, China*
[b] *School of Stomatology, Qingdao University, Qingdao 266003, China*
[c] *College of Materials Science and Engineering, Qingdao University, Qingdao 266003, China*
[d] *Department of Dental Materials and Prosthodontics, School of Dentistry of Ribeirao Preto, University of Sao Paulo, Ribeirao Preto, 14040904, SP, Brazil*
[e] *Applied Oral Sciences and Community Dental Care, Faculty of Dentistry, The University of Hong Kong, Hong Kong S.A.R., 999077, China*
[f] *University of Manchester, School of Medical Sciences, Oxford Road, M13 9PL Manchester, UK*
[g] *Department of Orthodontics, The Affiliated Hospital of Qingdao University, Qingdao, 266000, China*
[1] The first two named authors have contributed equally to the work.

[*] Corresponding authors.
Email addresses: quietfly_2018@163.com (J. Fu), wting8561@163.com (T. Wang)

Declarations of interest: none

Published in *Dental Materials* 2024; 40(4): 608-618

Abstract

Objective. The current dental resin composites often suffer from polymerization volumetric shrinkage, which can lead to microleakage and potentially result in recurring tooth decay. This study presents the synthesis of a novel monomer, (3,9-diethyl-1,5,7,11-tetraoxaspiro[5,5] undecane-3,9-diyl)bis(methylene) bis((2-(3-(prop-1-en-2-yl)phenyl)propan-2-yl)carbamate) (DDTU-IDI), and evaluates its effect in the formulation of low-shrinkage dental resin composites.

Methods. DDTU-IDI was synthesized through a two-step reaction route, with the initial synthesis of the required raw material monomer 3,9-diethyl-3,9-dihydroxymethyl-1,5,7,11-tetraoxaspiro-[5,5] undecane (DDTU). The structures were confirmed using Fourier-transform infrared (FT-IR) spectroscopy and hydrogen nuclear magnetic resonance (^{1}HNMR) spectroscopy. Subsequently, DDTU-IDI was incorporated into Bis-GMA-based composites at varying weight percentages (5, 10, 15, and 20 wt%). The polymerization reaction, degree of conversion, polymerization shrinkage, mechanical properties, physicochemical properties and biocompatibility of the low-shrinkage composites were thoroughly evaluated. Furthermore, the mechanical properties were assessed after a thermal cycling test with 10,000 cycles to determine the stability.

Results. The addition of DDTU-IDI at 10, 15, and 20 wt% significantly reduced the polymerization volumetric shrinkage of the experimental resin composites, without compromising the degree of conversion mechanical and physicochemical properties. Remarkably, at a monomer content of 20 wt%, the polymerization volumetric shrinkage was reduced to 1.83 ± 0.530%. Composites containing 10, 15, and 20 wt% DDTU-IDI exhibited lower water sorption and higher contact angle. Following thermal cycling, the composites exhibited no significant decrease in mechanical properties, except for the flexural properties.

Significance. DDTU-IDI has favorable potential as a component which could produce volume expansion and increase rigidity in the development of low-shrinkage dental resin composites. The development of low-shrinkage composites containing DDTU-IDI appears to be a promising strategy for reducing polymerization volumetric shrinkage, thereby potentially enhancing the longevity of dental restorations.

Keywords:

Polymerization shrinkage; Monomer; Resin composites; Physical properties; Thermocycling.

1. Introduction

Resin composites have gained wide acceptance and are extensively used in restorative dentistry. The development of modern dental composites started with Bowen's resin composites. Numerous studies have been conducted on resin composites, mainly focusing on modifications to their inorganic fillers [1-3] and organic matrices [4,5]. Since the 1960s, bisphenol A glycidyl methacrylate (Bis-GMA) has been the most commonly used base monomer in polymeric dental materials. It serves as the main organic component in commercial resin composites. Bis-GMA-based composites offer superior aesthetic quality and mechanical strength, along with low volatility and tissue diffusivity. However, the structure of Bis-GMA contains two hydroxyl groups, the formation of hydrogen bonds increases the water absorption and viscosity. Excessive water absorption may plasticize the matrix and promote hydrolytic degradation, contributed to the defective effects of the properties of composites [6]. The high viscosity of Bis-GMA can adversely affect the handling properties of the composites. A common solution to this issue is the incorporation of lower viscosity monomers, such as triethylene glycol dimethacrylate (TEGDMA) as diluents. However, it may introduce additional polymerization volumetric shrinkage [7]. Based on the difference in monomer density, the reactive group density of the monomer, and the degree of conversion achieved, the polymerization shrinkage of Bis-GMA is approximately 10%, while TEGDMA reaches around 17% [8]. Some properties of the chain-growth crosslinked polymerization of dimethacrylate dental formulations cannot be completely eliminated, often resulting in composites failure. In the process of covalent connection between monomers, the shortening of the van der Waals distance between two molecules (0.3 nm-0.5 nm) to the length of the covalent bond (0.15 nm) [9] leads to high shrinkage. It is in direct proportion to the functional group conversion and strongly associated with the desired increase in modulus. Furthermore, the instantaneous transition from liquid to solid is associated with early gelation, and the subsequent initiation of reaction-diffusion-controlled network formation hinders viscous flow in the later stages of polymerization [10]. The issue of polymerization shrinkage in composites remains a significant clinical problem, often leading to premature failure of composite restorations. This failure can manifest as microleakage and microbial accumulation, consequently causing sensitivity, staining, and secondary, or recurrent caries.

Extensive research has been conducted to mitigate the polymerization shrinkage of composites. Common strategies for achieving low polymerization volumetric shrinkage include the incorporation of expansion monomers, low-polymerization stress monomers and monomers with rigid chain segments [11]. Studies have shown that reducing the concentration of double bonds can lead to a decrease in polymerization shrinkage, which can be achieved by increasing the relative molecular weight or molar volume of monomers [12]. Moreover, in contrast to the free radical polymerization system, a cationic ring-opening monomer system was introduced. 3M ESPE developed a type of composite called "Filtek Silorane" which is entirely dependent on cationic ring-opening polymerization. The volumetric shrinkage was less than 1% [13].

However, this composite could only be used with a specific adhesive and did not offer a sufficient range of shades (essentially only one) to match teeth.

Since the introduction of double ring-opening polymerization in 1972 [14], a wide range of monomers based on bicyclic orthoesters (BOEs), spiro orthoesters (SOEs), and spiro orthocarbonates (SOCs) have been developed. They can effectively alleviate polymerization shrinkage in dental materials through ring-opening polymerization mechanisms. In recent years, there has been a significant interest in the utilization of expansion monomers as anti-shrinkage agents [15]. Among these, SOCs exhibit the most significant volume expansions, attributed to the relatively more flexible open-chain structure and the compactness of the bicyclic monomer [16].

While SOCs exhibit significant volumetric expansion, their standalone use as resin matrix systems can be challenging, as evidenced by the withdrawal of "Filtek Silorane" from the market. Therefore, SOCs is often introduced into dimethacrylate dental formulations. However, the direct incorporation of SOCs into Bis-GMA-based resin composites does not yield satisfactory co-polymerization. Some functionalized SOCs with double bonds have been studied. One approach is to synthesize SOCs with external double bonds, which facilitates the ring-opening polymerization of the SOCs [17]. Another approach involves introducing polymerizable groups such as acrylates into the structure of SOCs [18]. In this case, it is necessary to simultaneously use both free radical initiators and cationic initiators to achieve conversion of double bonds and the spiro groups. On the other hand, their incorporation into composites could lead to a deterioration of mechanical properties, limiting their application [19,20].

Excellent new monomer systems should strive to reduce polymerization shrinkage without compromising the mechanical properties of traditional composites. It is widely recognized that the favorable mechanical properties of Bis-GMA composites are attributed to the repetitive benzene ring structure. Benzene rings are renowned for their rigid structure, which can enhance the mechanical performance of the composites. He et al. [21] synthesized an organic monomer Bis-EFMA, which possessed four benzene ring structures. They discovered that the flexural strength of Bis-EFMA-based composites was superior to that of Bis-GMA-based composites.

In this study, a novel high molecular weight monomer, named DDTU-IDI ((3,9-diethyl-1,5,7,11-tetraoxaspiro[5.5]undecane-3,9-diyl)bis(methylene) bis((2-(3-(prop-1-en-2-yl)phenyl)propan-2-yl)carbamate)), was synthesized. This monomer incorporates a spiro structure and two benzene ring structures. The design aims to mitigate the impact of SOCs on the mechanical properties of composites, while capitalizing on the advantages of SOCs in reducing polymerization shrinkage. The theoretical mechanism of DDTU-IDI includes three aspects: (1) The spiro structure of DDTU-IDI undergoes ring-opening polymerization, resulting in volume expansions. (2) The high molecular weight of DDTU-IDI provides a low double-bond concentration. (3) The rigid structure benzene rings of DDTU-IDI help to maintain favorable mechanical properties. Therefore, the objective of this study is to synthesize a novel monomer DDTU-IDI and evaluate the performance of the new low-shrinkage dental resin composites containing DDTU-IDI. The assumptions of the study were: 1) DDTU-IDI can reduce the polymerization shrinkage and shrinkage stress of the experimental

resin composites. 2) The addition of DDTU-IDI will not affect the degree of conversion, mechanical and physicochemical properties of the experimental resin composites. 3) The experimental resin composites possess favorable resistance to aging. 4) The experimental resin composites show no cytotoxicity.

2.Materials and methods

2.1 Materials

1,1,1-Tris(hydroxymethyl)propane (TMP), dibutyltin oxide (DBTO), toluene, carbon disulfide (CS_2), n-Hexane and ethyl acetate were purchased from Sinopharm (Beijing, China). 3-isopropenyl-α, α-dimethylbenzyl isocyanate (IDI) and cationic initiator diphenyliodonium hexafluorphosphate (DPI) was purchased from Maclin (Shanghai, China). Dibutyltin dilaurate (DBTDL) and tetrahydrofuran were purchased from Energy (Shanghai, China). Bisphenol A glycidyl methacrylate (Bis-GMA), triethylene glycol dimethacrylate (TEGDMA), camphorquinone (CQ) and N, N-dimethylaminoethyl methacrylate (DMAEMA) were purchased from Sigma-Aldrich (St. Louis, MO, USA). Silanized barium borosilicated glass (BaBSi, 0.7 μm) was obtained from Esstech Inc (USA). All materials used were analytical reagents and did not require further purification before use. Dulbecco's modified Eagle's medium (DMEM) was purchased from Hyclone (Logan, UT, USA). Cell counting kit-8 (CCK-8) was purchased from Biosharp (Guangzhou, China).

2.2 Synthesis of DDTU

DDTU was synthesized following the route depicted in Fig. 1A. Initially, a mixture of TMP (26.834g), DBTO (49.787g), and 300 mL of toluene was placed in a three-necked round-bottom flask equipped. The reaction mixture was stirred and refluxed at 120°C until no water was produced. Subsequently, the reaction system was cooled to room temperature, and 16 mL of CS_2 was gradually added. The reaction mixture was then reheated to 100°C and continue to react for 12 h. After completion, the solvent was removed by vacuum distillation, and the resulting product was washed multiple times with n-hexane. Finally, the product was recrystallized using toluene and dried under vacuum at 60 °C for 24 h to obtain DDTU.

2.3 Synthesis of DDTU-IDI

DDTU-IDI was prepared by reacting one mole of DDTU with two moles of IDI, in the presence of DBTDL as a catalyst (Fig. 1B). The reaction mixture consisted of DDTU (0.05 mol), IDI (0.10 mol), 100 mL of anhydrous THF and 2 drops of DBTDL, which was stirred at 45°C. The reaction was allowed to proceed until the hydroxyl group of DDTU reacted completely with the isocyanate group of IDI. The completion of the reaction was confirmed by FT-IR analysis (the infrared absorbance peak corresponding to the -NCO group at 2250 cm^{-1} vanished). The THF solvent was then removed by vacuum distillation, and the resulting product was washed with n-hexane. For further purification, column chromatography was conducted using silica gel as the stationary phase and a mixture of ethyl acetate and n-hexane as the eluent.

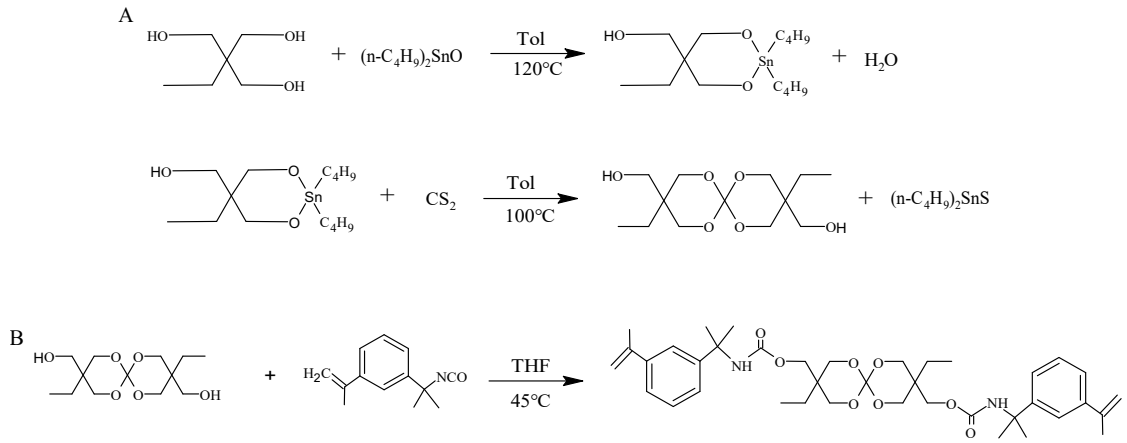

Fig. 1 - Synthesis routes of A. DDTU and B. DDTU-IDI.

2.4 Fabrication of experimental composites

The composition and proportions of the resin matrix for the experimental composites are provided in Table 1. The experimental composites were divided into five groups based on different mass ratios of DDTU-IDI in the resin matrix. Resin matrix in each group was placed in a light-protected container and stirred on a magnetic stirrer in the dark overnight until a homogeneous solution was obtained. Subsequently, the inorganic fillers (silanized BaBSi, 74 wt%) were gradually added to the resin matrix and mixed thoroughly using a SpeedMixer^{TM} (DAC150FVZ, Hauschild, Germany) at a speed of 1600 rpm/min. In addition, to evaluate their potential for clinical application, a commercial resin composite, CHARISMA (KULZER, Germany) was included as a commercial control, denoted as group C. CHARISMA is a kind of Bis-GMA based composite with inorganic fillers composed of barium aluminosilicate glass and silica dioxide.

Table 1 - Composition of resin matrix for experimental composites (wt%)

Group	Bis-GMA	TEGDMA	DDTU-IDI	CQ	DAMAEMA	DPI
D_0	70	30	0	1	2	2
D_5	67.5	27.5	5	1	2	2
D_{10}	63	27	10	1	2	2
D_{15}	59.5	25.5	15	1	2	2
D_{20}	56	24	20	1	2	2

Group D_0 ~ D_{20} refers to experimental composites containing 0~20 wt% DDTU-IDI. Bis-GMA: bisphenol A glycidyl methacrylate, TEGDMA: triethylene glycol dimethacrylate, DDTU-IDI: (3,9-diethyl-1,5,7,11-tetraoxaspiro[5,5]undecane-3,9-diyl)bis(methylene) bis((2-(3-(prop-1-en-2-yl)phenyl)propan-2-yl)carbamate), CQ: camphorquinone, DMAEMA: N, N-dimethylaminoethyl methacrylate. DPI: diphenyliodonium hexafluorphosphate.

2.5 Polymerization reaction and degree of conversion

In order to observe the changes of functional groups (including spiro structure and C=C) in composites before and after polymerization, and determine the degree of conversion (DC), a Fourier-transform infrared (FT-IR) spectrometer equipped with an attenuated total reflectance crystal (ATR) (Nicolet iS5, Thermo Scientific, USA) was utilized. The wave range of the instrument was set to 4000~500 cm^{-1}, with 32 scans and a 4 cm^{-1} resolution. Specimens (Φ 6 × 1 mm, n = 3) were cured for 20 s and then stored in air at 37°C for 24 h before FT-IR testing was conducted. The uncured pastes were also tested by FT-IR. DC was calculated by analyzing the aliphatic C=C peak at 1635 cm^{-1} and normalizing it against the aromatic C=C peak at 1605 cm^{-1} using the following formula [22,23]:

$$DC(\%) = (1 - \frac{R_{cured}}{R_{uncured}}) \times 100 \quad (1)$$

$$R = \frac{A_{1635}}{A_{1605}} \quad (2)$$

2.6 Polymerization volumetric shrinkage

According to the Archimedes principle, the polymerization volumetric shrinkage (VS) of the specimens was determined by measuring the density change of uncured and cured composites using an electronic densitometer (DX-120, China) [21]. The mass of the metal dish was measured in both air and distilled water. The density of the metal dish (ρ_m) was calculated using the following formula:

$$\rho_m = \frac{m_{ma}}{m_{ma} - m_{mw}} \rho_0 \quad (3)$$

where m_{ma} is the mass of the metal dish in air, m_{mw} is the mass of the metal dish in distilled water, ρ_0 is the density of distilled water.

Unpolymerized samples (n=5) were placed in a metal dish, and the combined mass of the metal dish and the sample was measured both in air and in distilled water. The density of the unpolymerized sample (ρ_{up}) was calculated by the following formula:

$$\rho_{up} = \frac{m_{uma} - m_{ma}}{m_{uma} - (\frac{m_{ma}\rho_0}{\rho_m}) - m_{umw}} \quad (4)$$

where m_{uma} and m_{umw} are the mass of the metal dish containing unpolymerized sample in air and in distilled water, respectively. ρ_m is the density of the metal dish. m_{ma} and ρ_0 are consistent with the previous representations.

The VS of the experimental composites was calculated according to the following formula:

$$VS = \frac{\rho_p - \rho_{up}}{\rho_p} \times 100\% \quad (5)$$

2.7 Polymerization shrinkage stress (SS)

The polymerization shrinkage stress (SS) was tested a universal testing machine (WDW-5E, Time Shijin, China) [13]. The cylindrical mold (Φ 4 × 2 mm, n = 5) was placed on the glass base and the uncured composites was evenly fill into the mold, above which was an organic glass rod. The bottom of the rod and the organic glass base that corresponds to the mold were polished with sandpaper. The specimen height was controlled at 2 mm by adjust the universal testing machine. A 400–500 nm LED light source (LED-B, Woodpecker, China) with an approximate intensity of 1000 mW/cm^2 to irradiate the composites from the bottom for 60 s. Simultaneously, record the development of resin stress over time. This process should be continued for 30 minutes, and the maximum value of stress within this time is recorded as the SS.

2.8 Specimen preparation

The preparation of the composites and fabrication of the specimens followed ISO 4049:2019 guidelines, which required a yellow light darkroom with a relative humidity ranging from 30% to 70% and an ambient temperature of (23 ± 1) °C. A white background glass plate was used, and the molds were placed on a 50 μm polyester film. The material was filled evenly into the mold, and a 50 μm polyester film and a 1 mm glass slide were placed on top. The glass slide was pressed uniformly to allow slight overflow of the material. The samples were then light-cured using a 400–500 nm LED light source (LED-B, Woodpecker, China) with an approximate intensity of 1000 mW/cm^2. Any rough edges or excess material were carefully removed by lightly sanding with sandpaper. After fabrication, the specimens were placed in a water bath maintained at 37°C for 24 h. The details of the tested samples were listed in Table Sl and Fig S1.

2.9 Mechanical properties

In this section, the specimens were divided into two parts. One part was tested after being immersed in a 37°C water bath for 24 h, denoted as unaged; while the other part underwent an aging experiment using a thermal cycling test machine, denoted aged. The specimens were subjected to cycles between 5°C and 55°C water baths, with each cycle consisting of a 20 s dwell time at each temperature. A total of 10,000 cycles were performed before testing. The evaluation of mechanical properties includes flexural properties, compressive strength (CS), diameter tensile strength (DTS), and vickers hardness (VH). More detailed testing information can be found in the Supporting Information.

2.10 Physicochemical properties

2.10.1 Depth of cure

According to ISO 4049:2019, a cylindrical metal mold (Φ 6 × 12 mm, n = 5) was utilized to uniformly fill the composite paste into the mold. Light-curing was applied

from the top for 20 s. Any remaining uncured resin was carefully and evenly removed using a plastic scraper. The thickness of the cured composite was measured using a digital caliper with an accuracy of 0.01 mm. The obtained thickness was divided by 2 to determine the depth of cure of the composites.

2.10.2 Water sorption (W_{sp}) and solubility (W_{sl})

According to ISO 4049:2019, the specimens were fabricated using a metal mold (Φ 15 × 1 mm, n = 5). After curing, the specimens were individually placed in a desiccator containing moisture-absorbing silica gel. The desiccator was placed in a 37°C drying oven for 22 h. Following this, the specimens were transferred to another desiccator with moisture-absorbing silica gel and maintained at 23 °C for 2 h. The specimens were subsequently weighed with an accuracy of 0.1 mg. This weighing process was repeated every 24 h and the mass of the specimens was recorded. Once the mass of the specimens reached a stable value (with a mass change of less than 0.1 mg/24 h), this mass was recorded as m_1.

The diameter and thickness of specimens were measured using a caliper (accurate to 0.01 mm). Based on these measurements, the volume (V) of the specimens were calculated. The specimens were then immersed in a 37°C ultrapure water bath for a duration of 7 d, with each specimen being submerged in at least 10 mL of distilled water. Care was taken to ensure that no overlapping occurred among the specimens. After the 7-day immersion period, the weights of the specimens were measured with a precision of 0.1 mg, denoted as m_2. The specimens were then subjected to the same procedure used to obtain m_1 and the resulting mass was recorded as m_3. W_{sp} and W_{sl} were figured using the following formulas:

$$W_{sp} = (m_2 - m_3) / V \quad (6)$$

$$W_{sl} = (m_1 - m_3) / V \quad (7)$$

2.10.3 Water contact angle

The static water contact angle of the samples (Φ 6 × 1 mm, n = 3) was measured using an optical contact angle measurement instrument (DSA30S, KRÜSS, Germany). Three measurements were taken for each sample at different positions. A volume of 2 μL of distilled water (Watsons, China) was dropped onto the surface of the sample. The equilibrium internal angle (°) between the tangent line on the liquid drop surface at the solid/liquid/gas three-phase interface and the horizontal baseline of the sample surface was recorded using a digital imaging camera.

2.11 Cytotoxicity

2.11.1. Preparation of composites extracts

Composites extracts were prepared according to ISO 10993-5 for in vitro cytotoxicity testing. Cured specimens (Φ 10 × 1 mm) was exposed to UV light for 60 min, followed by immersion in 75% alcohol for 30 min and rinsed three times with phosphate-buffered saline (PBS, solarbio, China). The sterilized samples were immersed in the DMEM medium and place them in a 37 °C incubator (with 5% CO_2 and 5% humidity) for 24

hours to obtain the sample extract. The ratio of the sample surface area to the volume of the culture medium is 1.25 cm^2/mL.

2.11.2. CCK-8 assay

Human gingival fibroblasts (HGFs) were used to evaluate the cytotoxicity of the composites extracts. The cells were obtained from the third molars of healthy volunteers (Ethical approval has been obtained from the Ethics Committee of Qingdao University Affiliated Hospital, QYFY WZLL 28422). The cell suspension with a density of 3×10^4 cells/mL was added to a 96-well plate, with 100 μL per well. The plate was then incubated in a 37 °C incubator (with 5% CO_2 and 5% humidity). After 24 hours, replace the culture medium with 100 μL of composites extract (experimental group) or 100 μL of DMEM (negative control) in each well. The plates were placed back into the incubator and incubated. On the 1 d, 3 d and 5 d, cultures were removed and 100μL of CCK-8 solution (10% CCK-8 reagent) was added. The cells were Incubated in a light-protected incubator for 5 h. Then, the OD values were measured using a microplate reader (Safire Ⅱ, TECAN, Austria) at a wavelength of 450 nm. The relative growth rates (RGR) of HGFs were calculated by the following formula:

$$RGR(\%) = \frac{OD_{\text{exprimental}}}{OD_{\text{negtive}}} \times 100\% \quad (8)$$

The cytotoxicity grading for cell viability was as follows [24]:
Grade 0, noncytotoxic: RGR > 90%.
Grade 1, slightly cytotoxic: RGR = 60 ~ 90%.
Grade 2, moderately cytotoxic: RGR = 30 ~ 59%.
Grade 3, severely cytotoxic: RGR ≤ 30%.

2.11 Statistical analysis

Statistical analysis was performed using GraphPad Prism version 9.5.0. To evaluate the statistical differences among the groups, One-way analysis of variance (ANOVA) followed by Tukey's multiple comparison test was conducted. A t-test (Holm-Sidak) method was used to assess the difference between unaged and aged specimens within each group for the mechanical tests. A significance level of $p < 0.05$ was considered to indicate a statistically significant difference among the groups.

3.Results

3.1 Characterizations of DDTU

The chemical structure of DDTU was confirmed by FT-IR and ^{1}HNMR. In the FT-IR spectrum of DDTU (Fig. 2A), absorption peaks of hydroxyl groups could be observed at 3567 cm^{-1} and 3382 cm^{-1}; the peaks around 2878 cm^{-1} was due to the saturated hydrocarbon C-H stretching vibration, and the peaks from 1361 cm^{-1} to 1453 cm^{-1} was due to the C-H bending vibration, indicating the presence of -CH_3 and -CH_2; the peaks at 1011 cm^{-1} and 1184 cm^{-1} were C-O stretching vibration peaks; the characteristic absorption peak of the spiro group could be observed around 1221 cm^{-1}. The ^{1}HNMR spectrum (Fig. 2B) showed typical peaks corresponding to all the protons

in the DDTU structure. ^{1}HNMR (600 MHz, C_3D_6O) δ(ppm): 3.6-3.8 (m, 12H), 2.7 (s, 2H), 1.31-1.42 (m, 4H), 0.81-0.86 (m, 6H). DDTU was obtained as a white powder with a yield of 68.7%.

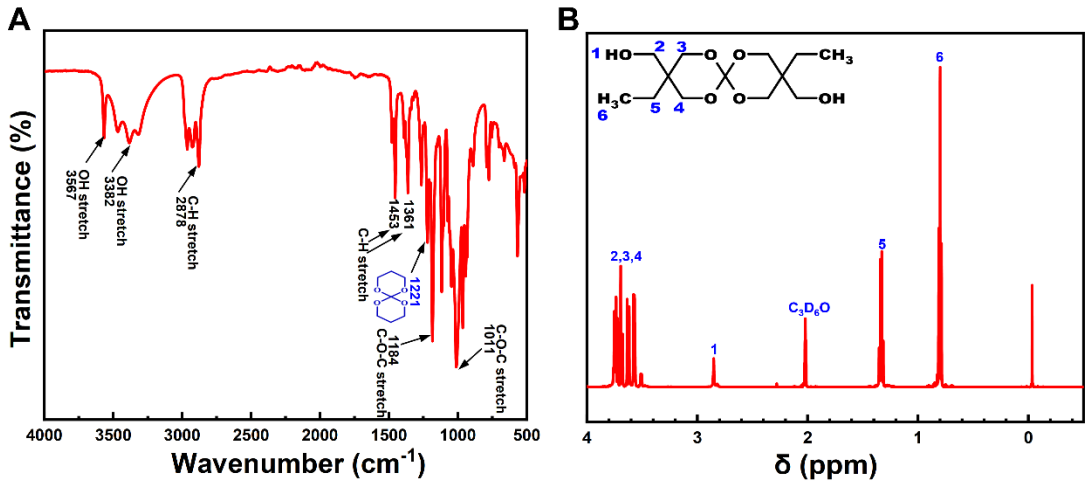

Fig. 2 - A. FT-IR spectrum of DDTU. B. ^{1}HNMR spectrum of DDTU.

3.2 Characterizations of DDTU-IDI

According to the FT-IR spectrum of the reaction mixture of DDTU and IDI before and after the reaction, as shown in Fig. S2. It can be observed that the infrared peak corresponding to the isocyanate (-NCO) functional group in the reaction mixture disappeared after the reaction, indicating the completion of the reaction.

The FT-IR spectrum and ^{1}HNMR spectrum of DDTU-IDI are shown in Fig. 3B and Fig. 3C, respectively. The FT-IR spectrum of DDTU-IDI exhibited absorption peaks corresponding to aliphatic C=C bonds and aromatic C=C bonds at 1635 cm^{-1} and 1605 cm^{-1}, respectively. The C=O peak was observed at 1698 cm^{-1}. Additionally, the characteristic absorption peak of the spiro structure was observed around 1221 cm^{-1}. The ^{1}HNMR spectrum showed distinct signals corresponding to different protons in DDTU-IDI. ^{1}HNMR (600 MHz, C_3D_6O) δ(ppm): 7.2-7.6 (m, 8H), 6.7 (s, 2H), 5.0, 5.5 (s, 4H), 3.2-4.2 (m, 12H), 2.1 (s, 6H), 1.6 (s, 12H), 1.3 (s, 4H), 0.8 (s, 6H). DDTU-IDI was obtained as a white powder with a yield of 58%.

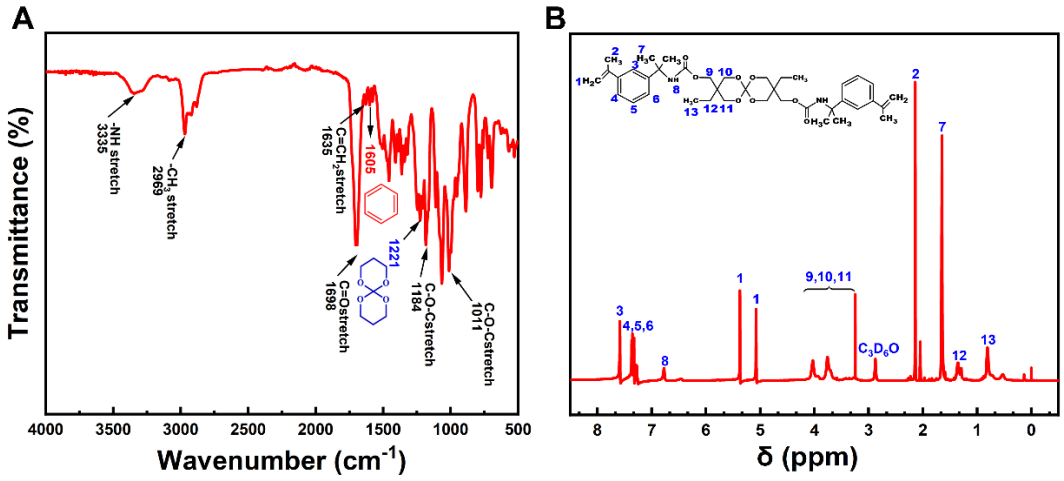

Fig. 3 - A. FT-IR spectrum of DDTU-IDI. B. ^{1}HNMR spectrum of DDTU-IDI.

3.3 Polymerization reaction and degree of conversion

Fig. 4A displays the FT-IR spectrum of the composites containing 20 wt% DDTU-IDI before and after curing. The peak intensity of the aromatic C=C (1605 cm^{-1}) remained relatively constant, indicating minimal changes, while a decrease was observed in the peak intensity of the aliphatic C=C (1635 cm^{-1}) and spiro structure (1221 cm^{-1}), confirming the occurrence of the polymerization reaction and the ring opening of the spiro structure. As shown in Fig. 4B, no significant differences were observed in the degree of conversion (DC) among the groups D_0 ~ D_{20}. The DC of these groups was 71.79 ± 3.402 %, which was significantly higher than that of group C (60.43 ± 0.940 %) ($p < 0.05$).

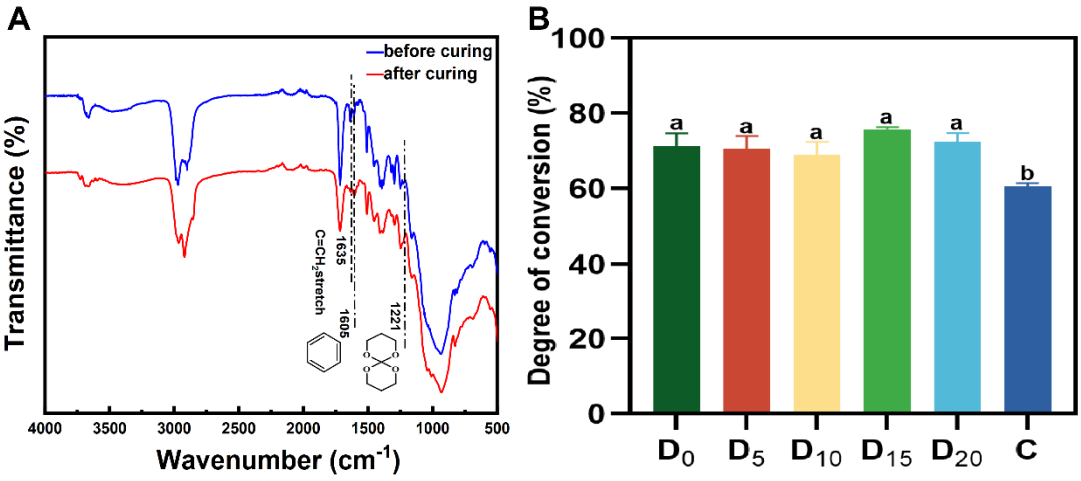

Fig. 4 - A. FT-IR spectrum of composites containing 20 wt% DDTU-IDI before and after curing. B. Degree of conversion of experimental composites. Different letters indicate statistical difference ($p < 0.05$). Group D_0 ~ D_{20} refers to experimental composites containing 0~20 wt% DDTU-IDI, while group C represents the commercial control.

3.4 Polymerization volumetric shrinkage (VS)

The result of polymerization volumetric shrinkage is shown in Fig. 5A. Among groups D_0 ~ D_{20}, the VS showed a decreasing trend with the addition of DDTU-IDI. The VS of groups D_{10} ~ D_{20} were significantly lower than that of group D_0 and group C ($p < 0.05$). Notably, group D_{20} exhibited the lowest VS, measuring at 1.83 ± 0.530%.

3.5 Polymerization shrinkage stress (SS)

Fig. 5B showed the polymerization shrinkage stress of composites., The SS showed a decreasing trend with the addition of DDTU-IDI among groups D_0 ~ D_{20}. The SS of groups D_{15} ~ D_{20} were significantly lower than that of group D_0 and group C ($p < 0.05$).

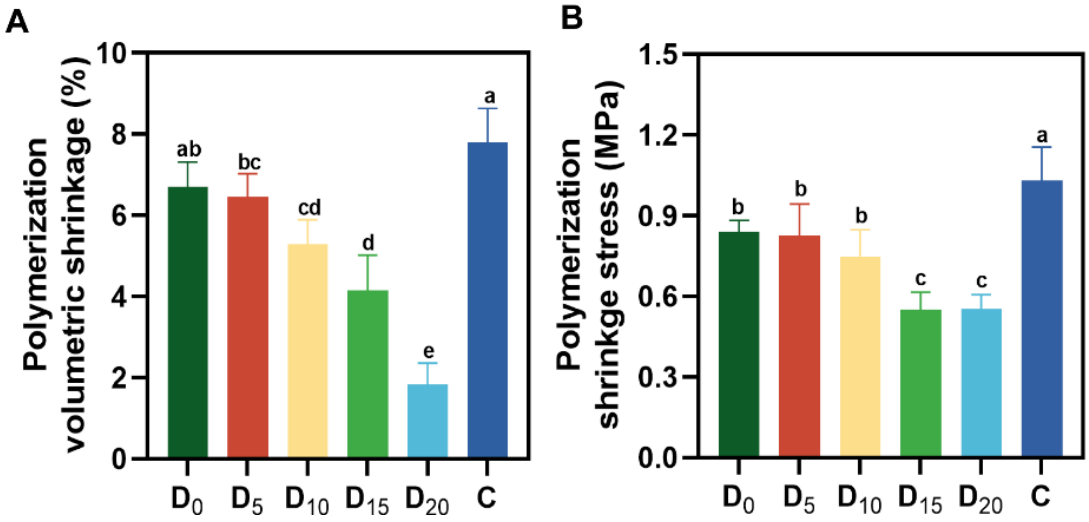

Fig. 5 - Polymerization volumetric shrinkage (A) and polymerization shrinkage stress (B) of experimental composites. Different letters indicate statistical difference ($p < 0.05$). Group D_0 ~ D_{20} refers to experimental composites containing 0~20 wt% DDTU-IDI, while group C represents the commercial control.

3.6 Mechanical properties

The mechanical properties of experimental composites are illustrated in Fig. 6. There were no statistically significant differences in the mechanical properties of the experimental composites between group D_0 and groups D_5 ~ D_{20}. The FS of groups D_0 ~ D_{15} was significantly higher than group C ($p < 0.05$), while the FM and VH of groups D_0 ~ D_{20} were significantly higher than group C ($p < 0.05$).

The specimens were further divided into two groups: unaged and aged, based on whether they had undergone the thermocycling regimen of 10,000 cycles. The mechanical properties of unaged and aged composites were then compared. There were no statistically significant differences in the VH, CS, and DTS between the unaged and aged composites within each group. However, post-aging, there was a decrease in the FS for all groups, as well as a decrease in the FM for groups D_5 ~ D_{20} and in the RM for group C and groups D_0 ~ D_{10} ($p < 0.05$). In the aged composites, groups D_0 ~ D_{20} exhibited significantly higher FM and VH compared to group C ($p < 0.05$). Additionally, groups D_{15} and D_{20} showed significantly higher CS compared to group D_0 and group C ($p < 0.05$). The fractured surface morphology of aged and unaged composites from the

three-point bending test are shown in Fig. 7 and Fig. 8. For each group, the fractured morphology of the aged composites displayed rougher surfaces and exhibited more cracks and gaps (indicated by white arrows) compared to the unaged composites.

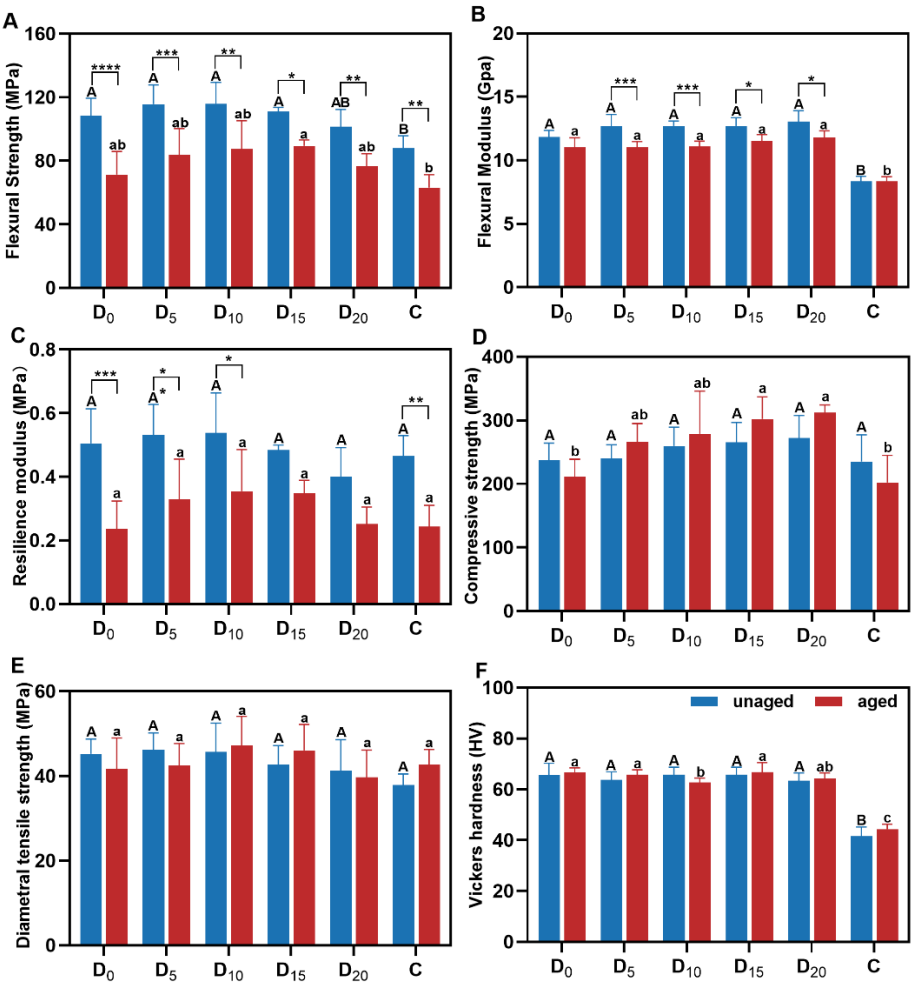

Fig. 6 - Mechanical properties of experimental composites. A. Flexural strength. B. Flexural modulus. C. Resilience modulus. D. Compressive strength. E. Diametral tensile strength. F. Vickers hardness. Unaged: specimens tested at 24 h. Aged: specimens tested after undergoing 10,000 thermocycles. Significant difference: *$p < 0.05$, **$p < 0.01$, ***$p < 0.001$. The uppercase letters above the horizontal line indicate the difference between unaged composites. The lowercase letters above the horizontal line indicate the difference between aged composites. Different uppercase letters or different lowercase letters indicate statistical difference ($p < 0.05$). Group $D_0 \sim D_{20}$ refers to experimental composites containing 0~20 wt% DDTU-IDI, while group C represents the commercial control.

3.7 Physicochemical properties

The physicochemical properties of the composites are depicted in Fig. 7. Significant differences in the depth of cure were observed between the groups $D_{10} \sim D_{20}$ and groups $D_0 \sim D_5$ ($p < 0.05$). The addition of DDTU-IDI led to a decreasing trend in the W_{sp} of the composites, with D_{20} exhibiting the lowest value. There were no statistically

significant differences in the W_{sl} among groups D_0 ~ D_{20}. The water contact angle of the groups D_{10} ~ D_{20} consistently exhibited higher values compared to the group C and groups D_0 ~ D_5 ($p < 0.05$), and as the DDTU-IDI content increased, there was an upward trend in the water contact angle of composites.

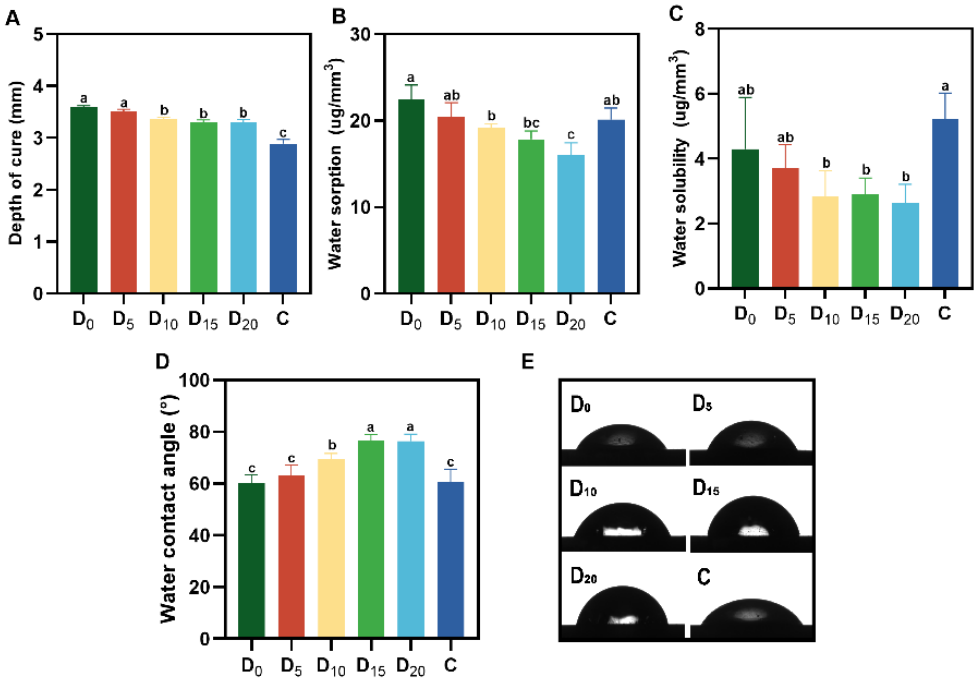

Fig. 7 - Physicochemical property of experimental composites. A. Depth of cure. B. Water sorption. C. Water solubility. D. Water contact angle. E. Images of water contact water. Different letters indicate statistical difference ($p < 0.05$). Group D_0 ~ D_{20} refers to experimental composites containing 0~20 wt% DDTU-IDI, while group C represents the commercial control.

3.8 Cytotoxicity

Fig. 8 shows the Relative Growth Rate (RGR) of cells cultured with the composites extracts for 1, 3, and 5 days. There were no statistically significant differences ($p > 0.05$) in the RGR scores among all groups at each time point. The RGR scores of all groups were above 90% (Grade 0).

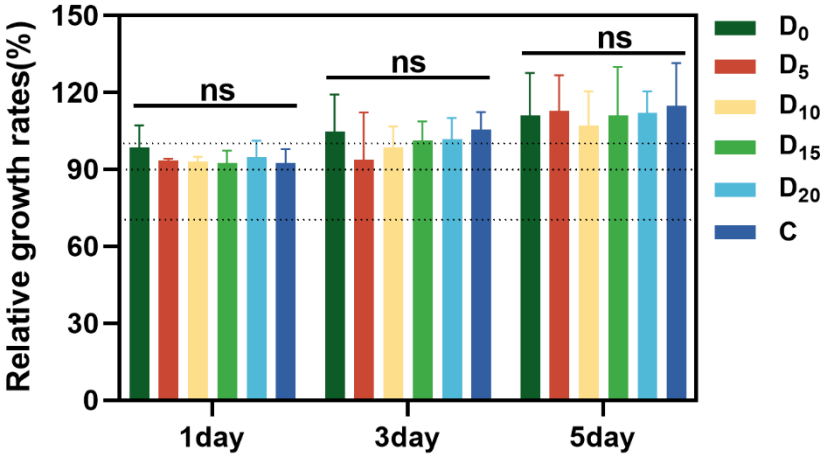

Fig. 8 - The relative growth rates of HGF cells for 1 d, 3 d and 5 d. Ns: no statistically significant difference ($p > 0.05$). Group $D_0 \sim D_{20}$ refers to experimental composites containing 0~20 wt% DDTU-IDI, while group C represents the commercial control.

4. Discussion

The performance of composites is significantly influenced by the structure and chemical properties of the monomers. Hence, the design of specific monomers holds great importance in enhancing the properties of composites. In this study, DDTU-IDI was specifically designed with a spiro structure and two benzene ring structures to mitigate the polymerization volumetric shrinkage of the composites while maintaining favorable mechanical properties.

The synthesis of DDTU-IDI primarily involved the direct reaction between the -OH group of DDTU and the -NCO group of IDI. The reaction was monitored using FT-IR. The reaction was considered complete when the characteristic infrared peak corresponding to the isocyanate (-NCO) functional group in the reaction mixture disappeared. The successful synthesis of DDTU-IDI was confirmed through the presence of spiro group, aliphatic C=C bonds and aromatic C=C bonds characteristic peaks of functional groups in the FT-IR spectrum and corresponding proton signals in the ^{1}HNMR spectrum. Furthermore, in the FT-IR analysis of DDTU-IDI, the absence of isocyanate functional group which is present in the raw material, provided further evidence supporting the formation of DDTU-IDI.

The degree of conversion for composites is one of the main factors determining its mechanical properties and polymerization volumetric shrinkage [25]. Composites with a higher degree of conversion exhibit higher crosslinking densities and more compact internal structures, which can enhance the mechanical properties and biocompatibility of the materials [26,27]. The visible light initiation system is of great importance in the polymerization of composites. The camphorquinone (CQ)/amine photopolymerization system is currently the most widely used light-curing dental restorative system, which belongs to the free radical initiation system. If the SOCs does not have external double

bonds, the addition of SOCs to resin composites cannot produce good co-polymerization by free radical initiator alone. Diaryliodonium salts exhibit good intermiscibility with other monomers, low nucleophilicity, high polymerization activity, and can maintain stability under room temperature. DPI, a type of diaryliodonium salt, can release both radical cations and free radicals upon the formation of cationic active centers. It has been reported that three-component photoinitiator system consisting of chromone, amine, and diaryliodonium salts can effectively initiate the polymerization of acrylic resins under visible light [28].

According to the FT-IR spectrum of the composites before and after curing, the observed changes in the peaks corresponding to the saturated hydrocarbon C-H stretching vibration (around 2969 cm^{-1}) and the unsaturated C-H stretching vibration (around 3000 cm^{-1}) indicate the formation of an interpenetrating polymer network (IPN). Additionally, the decrease in peak intensity of the aliphatic C=C (1635 cm^{-1}) and spiro structure (1221 cm^{-1}) further confirms the presence of an IPN and the ring-opening of the spiro structure. It is noteworthy that the addition of DDTU-IDI did not negatively impact the degree of conversion of the composites. In fact, the low-shrinkage composites containing DDTU-IDI exhibited a better degree of conversion compared to the commercial control.

As anticipated, the addition of DDTU-IDI resulted in a reduction in the VS of the composites. As the proportion of DDTU-IDI increased, the experimental composites exhibited a decreasing trend in VS. When the addition of DDTU-IDI reached 20 wt%, the polymerization volumetric shrinkage of the composites decreased to 1.83 ± 0.530%. This reduction in VS can be attributed to two main factors. On the one hand, the spiro structure, through ring-opening polymerization mechanisms, could generate volume expansion during the polymerization process. More precisely, for every newly formed covalent bond, there was a transition from van der Waals distance to covalent distance, involving the breaking of two covalent bonds and a transition from covalent distance to near van der Waals distance [14]. This mechanism could partially compensate for the VS. The expansion capability of the monomer is influenced by the number of open rings per unit volume and the size of the rings [29]. DDTU-IDI includes two six-membered rings, which significantly reduces the VS of the resin composites. On the other hand, the decrease of VS may be attributed to the higher relative molecular weight of DDTU-IDI (Mw = 678 g mol^{-1}) compared to Bis-GMA (Mw = 512 g mol^{-1}) and TEGDMA (Mw = 286 g mol^{-1}). Sun et al. [30] synthesized the monomers BEF-EA (Mw = 596.67 g mol^{-1}) and BEF-GMA (Mw = 624.73 g mol^{-1}), which have higher molecular weights than Bis-GMA (Mw = 512.59 g mol^{-1}). They observed that composites based on these monomers exhibited lower VS compared to Bis-GMA-based composites under comparable double bond conversion rates. Similar results were obtained in this study. This may be attributed to the fact that when DDTU-IDI was incorporated into the Bis-GMA-based composites, it partially replaced Bis-GMA and TEGDMA, resulting in a decrease in the concentration of double bonds. This ultimately contributed to the observed VS [29]. The SS of the experimental groups decreased with the addition of DDTU-IDI, consistent with the result of VS. Group D_{15} and group D_{20} exhibited lowest SS. Shrinkage stress unlike polymerization shrinkage, it is not a material property, it is

the result of multiple factors. Factors such as the compliance of the testing systems, the elastic modulus, geometry, and mass of restorations could influence the SS [28].

The mechanical properties of composites play a crucial role, especially in areas exposed to chewing loads. The introduction of certain novel monomers has been found to potentially impact the mechanical properties of resin composites [20,31-34]. Duarte et al. [35] synthesized two novel monomers with spiro structures, which significantly reduced the polymerization volumetric shrinkage of the resin composites. However, these monomers also resulted in a decrease in the flexural strength of the composites. In contrast, the incorporation of DDTU-IDI, which includes a spiro structure, did not adversely affect the mechanical properties of the composites, which was consistent with the results of the degree of conversion. This may be attributed to the presence of two benzene rings in the structure of DDTU-IDI. The benzene ring, known for its rigid structure, which can enhance the physical and mechanical properties [36,37].

To evaluate the material's resistance to artificial aging conditions, an aging protocol involving 10,000 thermal cycles was employed. This protocol aims to simulate the thermal variations associated with eating, drinking and respiration. In the oral cavity, restorative materials are exposed to daily thermal cycling during the consumption of beverages and food. ISO 11405 recommends the use of 500 thermal cycles between 5°C and 55°C to simulate the short-term aging of dental materials [38]. It has been suggested that subjecting materials to 10,000 cycles can simulate approximately one year of clinical service [39,40]. From the conducted tests, it can be concluded that thermal cycling did not significantly impact the CS, VH and DTS of the composites while had a impact on flexural properties. In general, the effects of thermal cycling on composites can be attributed to two factors: temperature changes and water penetration. On the one hand, water infiltration can lead to hydrolysis of the silane coupling agent at the filler-matrix interface, disrupting the bonding between the filler and matrix interface [41]. On the other hand, the mismatch in coefficients of thermal expansion between the composite matrix and filler particles generates internal stresses within the material. These stresses can result in the formation of internal cracks, compromising the chemical bonding between the filler and composite matrix, and subsequently reducing the flexural strength and Weibull modulus of the resin composites [42]. Therefore, the flexural properties of the composites was somewhat compromised after thermal cycling. Interestingly, as the content of DDTU-IDI increased, the decreasing trend in the flexural performance of the resin became less pronounced. These findings help to predict the performance and durability of the composites in real-world clinical settings.

The depth of cure of resin composites is influenced by multiple factors, such as refractive index of the filler particles and resin matrix, photoinitiator type and its concentration, among others [43]. When the content of DDTU-IDI reached 10 wt%, the depth of cure of the composites decreased. The decrease in depth of cure is speculated to be due to the difference in the refractive index of DDTU-IDI, whcih further verification is required. However, it is crucial to note that the depth of cure for all the composites met the requirements of ISO 4049, and the depth of cure of experimental composites was higher compared to the commercial control.

Water sorption (W_{sp}) and solubility (W_{sl}) are crucial parameters for evaluating the performance of composites. The former indicates the amount of water absorbed by the material, and the latter represents the quantity of unreacted monomers released from the polymer network. In clinical practice, it is important to maintain low levels of W_{sp} and W_{sl} as water intrusion into materials and the release of monomers can have adverse effects on both the materials and the patient. Besides, a slight W_{sp} can contribute to compensating for polymerization volumetric shrinkage to some extent [44]. The experimental composites maintained low water absorption and solubility values and meet the ISO 4049 ($\leqslant$40 μg/mm^3 and $\leqslant$7.5μg/mm^3). The hydrophobic characteristics of the material is beneficial for clinical applications. This is because hydrophobic surfaces are more likely to detach biofilms, bacteria adhered to hydrophobic surfaces are more prone to detachment under the shear forces exerted by saliva fluid flow [45]. Water sorption of composites is influenced by the network structure of the polymer and the hydrophobicity of the polymer. Polymers with high hydrophobicity and high cross-linking density tend to have lower water sorption. Similarly, high water contact angle is associated with hydrophobicity. The composites containing 10~20 wt% DDTU-IDI exhibited lower water sorption and higher water contact angle, indicating higher hydrophobicity. The higher hydrophobicity of D_{10} ~ D_{20} may be attributed to the presence of urethane groups. Kerby et al. [46] reported that urethane dimethacrylate (UDMA)-based composites containing urethane groups have lower water sorption compared to Bis-GMA-based composites containing highly polar ether linkages and hydroxyl groups. On the other hand, DDTU-IDI lacks hydroxyl group (-OH) groups compared to Bis-GMA, which resulted in the composites containing DDTU-IDI being more hydrophobic. Because -OH group is a kind of hydrophilic functional group. Monomers containing OH groups tend to adsorb more water molecules [47]. Therefore, these results indicate that the composites containing 10~20 wt% are more suitable for long-term clinical applications.

In this study, the cytotoxic effects of composites extracts on human gingival fibroblasts (HGFs) were evaluated using the CCK-8 assay. The relative growth rates (RGRs) of the cells were measured on days 1, 3, and 5, respectively. Composites extracts of each group showed no cytotoxicity on HGFs cells. The impact of unpolymerized monomers in the extraction solution on cells may be more pronounced during the early stages of cell proliferation [20]. Furthermore, in all groups and at all time points, the RGR score were above 70%. According to the ISO 10993-5:2021, a decrease in cell viability of less than 30% indicates minimal or no cytotoxicity. The nontoxicity of the experimental composites was related to the formation of favourable IPN network, which could decrease the number of unpolymerized monomers. It is important for the long-term cytotoxicity properties of composites.

In conclusion, the assumptions were established. The addition of DDTU-IDI at 10~20 wt % effectively reduced the polymerization volumetric shrinkage of the experimental resin composites without compromising their mechanical properties and exhibited more improved hydrophobicity. Additionally, the experimental resin composites exhibited favorable resistance to aging and biocompatibility. These findings support the use of DDTU-IDI as an effective approach to minimize the polymerization

volumetric shrinkage of resin composites and potentially extend the lifespan of dental restorations.

5. Conclusion

In this study, a novel monomer, DDTU-IDI, was synthesized successfully and utilized in the preparation of the low-shrinkage resin composites without negatively impacting the degree of conversion. The composites containing 10 wt% ~ 20 wt% DDTU-IDI exhibit low polymerization shrinkage and shrinkage stress, desirable mechanical properties, favorable physicochemical properties and biocompatibility. Furthermore, they demonstrated favorable resistance to aging during thermal cycling. The novel dental resin composite system composed of the low shrinkage monomer DDTU-IDI may be a promising dental restoration that could reduce the onset of secondary caries.

References

[1] Tian J, Wu Z, Wang Y, Han C, Zhou Z, Guo D, et al. Multifunctional dental resin composite with antibacterial and remineralization properties containing nMgO-BAG. J Mech Behav Biomed Mater 2023;141:105783. https://doi.org/10.1016/j.jmbbm.2023.105783
[2] Wang Y, Wu Z, Wang T, Tian J, Zhou Z, Guo D, et al. Antibacterial and physical properties of resin cements containing MgO nanoparticles. J Mech Behav Biomed Mater 2023;142:105815. https://doi.org/10.1016/j.jmbbm.2023.105815
[3] Wu Z, Xu H, Xie W, Wang M, Wang C, Gao C, et al. Study on a novel antibacterial light-cured resin composite containing nano-MgO. Colloids and Surfaces B: Biointerfaces 2020;188:110774. https://doi.org/10.1016/j.colsurfb.2020.110774
[4] He J, Garoushi S, Säilynoja E, Vallittu P K, Lassila L. The effect of adding a new monomer “Phene” on the polymerization shrinkage reduction of a dental resin composite. Dent Mater 2019;35:627-35. https://doi.org/10.1016/j.dental.2019.02.006
[5] Aminoroaya A, Neisiany R E, Khorasani S N, Panahi P, Das O, Madry H, et al. A review of dental composites: Challenges, chemistry aspects, filler influences, and future insights. Compos Part B Eng 2021;216:108852. https://doi.org/10.1016/j.compositesb.2021.108852
[6] Fong H, Dickens S H, Flaim G M. Evaluation of dental restorative composites containing polyhedral oligomeric silsesquioxane methacrylate. Dent Mater 2005;21:520-9. https://doi.org/https://doi.org/10.1016/j.dental.2004.08.003
[7] Wang X, Huyang G, Palagummi S V, Liu X, Skrtic D, Beauchamp C, et al. High performance dental resin composites with hydrolytically stable monomers. Dent Mater 2018;34:228-37. https://doi.org/10.1016/j.dental.2017.10.007
[8] Barszczewska-Rybarek I M, Chrószcz M W, Chladek G. Novel Urethane-Dimethacrylate Monomers and Compositions for Use as Matrices in Dental Restorative Materials. Int J Mol Sci 2020;21:2644. https://doi.org/10.3390/ijms21072644
[9] Pulido C, Arrais C A G, Gomes G M, Franco A P G B, Kalinowski H J, Dávila-Sánchez A, et al. Kinetics of polymerization shrinkage of self-adhesive and conventional dual-polymerized resin luting agents inside the root canal. J Prosthet Dent 2021;125:535-42. https://doi.org/10.1016/j.prosdent.2020.01.017
[10] Podgórski M, Becka E, Claudino M, Flores A, Shah P K, Stansbury J W, et al. Ester-free thiol–ene dental restoratives—Part B: Composite development. Dent Mater 2015;31:1263-70. https://doi.org/https://doi.org/10.1016/j.dental.2015.08.147
[11] Fugolin A P P, Pfeifer C S. New Resins for Dental Composites. J Dent Res 2017;96:1085-91. https://doi.org/10.1177/0022034517720658
[12] Wang Z, Zhang X, Yao S, Zhao J, Zhou C, Wu J. Development of low-shrinkage dental adhesives via blending with spiroorthocarbonate expanding monomer and unsaturated epoxy resin monomer. J Mech Behav Biomed Mater 2022;133:105308. https://doi.org/10.1016/j.jmbbm.2022.105308
[13] Weinmann W, Thalacker C, Guggenberger R. Siloranes in dental composites. Dent Mater 2005;21:68-74. https://doi.org/10.1016/j.dental.2004.10.007

[14] Endo T, Bailey W J. Synthesis and radical ring-opening polymerization of spiro o-carbonates. Journal of Polymer Science: Polymer Chemistry Edition 1975;13:2525-30. https://doi.org/10.1002/pol.1975.170131110
[15] Marx P, Wiesbrock F. Expanding monomers as anti-shrinkage additives. Polymers (Basel) 2021;13:806. https://doi.org/10.3390/polym13050806
[16] Fu J, Liu W, Hao Z, Wu X, Yin J, Panjiyar A, et al. Characterization of a low shrinkage dental composite containing bismethylene spiroorthocarbonate expanding monomer. Int J Mol Sci 2014;15:2400-12. https://doi.org/10.3390/ijms1502240
[17] Stansbury J W, Bailey W J, Evaluation of Spiro Orthocarbonate Monomers Capable of Polymerization with Expansion as Ingredients in Dental Composite Materials. Progress in Biomedical Polymers 1990;133-9. https://doi.org/10.1007/978-1-4899-0768-4_14
[18] Stansbury J W, Ring-Opening Polymerization of a 2-Methylene Spiro Orthocarbonate Bearing a Pendant Methacrylate Group. American Chemical Society 1993; 540: https://doi.org/171-83. 10.1021/bk-1994-0540.ch014
[19] Yoo S H, Kim C K. Synthesis of a novel spiro orthocarbonate containing bisphenol-a unit and its application to the dental composites. Macromol Res 2010;18:1013-20. https://doi.org/10.1007/s13233-010-1005-z
[20] Berlanga Duarte M L, Reyna Medina L A, Torres Reyes P, Esparza González S C, Herrera González A M. Dental restorative composites containing methacrylic spiroorthocarbonate monomers as antishrinking matrixes. J Appl Polym Sci 2019;136:47114. https://doi.org/10.1002/app.47114
[21] Zhang X, Ma X, Liao M, Liu F, Wei Q, Shi Z, et al. Properties of Bis-GMA free bulk-filled resin composite based on high refractive index monomer Bis-EFMA. J Mech Behav Biomed Mater 2022;134:105372. https://doi.org/10.1016/j.jmbbm.2022.105372
[22] González-López J A, Fonseca-García A, Acosta-Ortiz R, Betancourt-Galindo R, Martínez-Ruiz E, Treviño-Martínez M E. Photopolymerizable dental composite resins with lower shrinkage stress and improved hydrolytic and hygroscopic behavior with a urethane monomer used as an additive. J Mech Behav Biomed Mater 2022;130:105189. https://doi.org/https://doi.org/10.1016/j.jmbbm.2022.105189
[23] He J W, Soderling E, Lassila L V, Vallittu P K. Preparation of antibacterial and radio-opaque dental resin with new polymerizable quaternary ammonium monomer. Dent Mater 2015;31:575-82. https://doi.org/10.1016/j.dental.2015.02.007
[24] Wang Y, Wu Z, Wang T, Tang W, Li T, Xu H, et al. Bioactive Dental Resin Composites with MgO Nanoparticles. ACS Biomater Sci Eng 2023;9:4632-45. https://doi.org/10.1021/acsbiomaterials.3c00490
[25] Xu T, Li X, Wang H, Zheng G, Yu G, Wang H, et al. Polymerization shrinkage kinetics and degree of conversion of resin composites. Journal of Oral Science 2020;62:275-80. https://doi.org/10.2334/josnusd.19-0157
[26] Pei X, Wang J, Cong Y, Fu J. Recent progress in polymer hydrogel bioadhesives. Journal of Polymer Science 2021;59:1312-37. https://doi.org/10.1002/pol.20210249
[27] Goldberg M. In vitro and in vivo studies on the toxicity of dental resin components: a review. Clin Oral Investig 2008;12:1-8.

https://doi.org/10.1007/s00784-007-0162-8
[28] Liu W, Fu J, Wu X, Ma Y, Liu X, Liao Y, et al. Influences of iodonium salts on the properties of a hybrid composite resin containing BisS-GMA and expanding monomer modified epoxy. Journal of Wuhan University of Technology-Mater Sci Ed 2015;30:1184-90. https://doi.org/10.1007/s11595-015-1293-4
[29] He J, Liao L, Liu F, Luo Y, Jia D. Synthesis and characterization of a new dimethacrylate monomer based on 5,5′ -bis(4-hydroxylphenyl)-hexahydro-4,7-methanoindan for root canal sealer application. J Mater Sci 2010;21:1135-42. https://doi.org/10.1007/s10856-009-3979-7
[30] Sun Y, Sun L, Hong L, Li J, Tang S, Zhao C. Bio-based non-estrogenic dimethacrylate dental composite from cloves. J Dent Res 2022;101:1613-9. https://doi.org/10.1177/00220345221109498
[31] Sarosi C, Moldovan M, Soanca A, Roman A, Gherman T, Trifoi A, et al. Effects of monomer composition of urethane methacrylate-based resins on the C=C degree of conversion, residual monomer content, and mechanical properties. Polymers 2021;13:4415. https://doi.org/doi: 10.3390/polym13244415.
[32] Fugolin A P, de Paula A B, Dobson A, Huynh V, Consani R, Ferracane J L, et al. Alternative monomer for BisGMA-free resin composites formulations. Dent Mater 2020;36:884-92. https://doi.org/10.1016/j.dental.2020.04.009
[33] He J, Söderling E, Lassila L V J, Vallittu P K. Synthesis of antibacterial and radio-opaque dimethacrylate monomers and their potential application in dental resin. Dent Mater 2014;30:968-76. https://doi.org/10.1016/j.dental.2014.05.013
[34] Fu W, Wang L, He J. Evaluation of mechanical properties and shrinkage stress of thiol-ene-methacrylate dental composites with synthesized fluorinated allyl ether. J Mech Behav Biomed Mater 2019;95:53-9. https://doi.org/10.1016/j.jmbbm.2019.03.027
[35] Duarte M L B, Medina L A R, Reyes P T, Gonzalez S C E, Gonzalez A M H. Dental restorative composites containing methacrylic spiroorthocarbonate monomers as antishrinking matrixes. J Appl Polym Sci 2019;136:10. https://doi.org/10.1002/app.47114
[36] Peutzfeldt A. Resin composites in dentistry: the monomer systems. Eur J Oral Sci 1997;105:97-116. https://doi.org/10.1111/j.1600-0722.1997.tb00188.x
[37] Kumar S R, Bhat I K, Patnaik A. Novel dental composite material reinforced with silane functionalized microsized gypsum filler particles. Polym Compos 2017;38:404-15. https://doi.org/10.1002/pc.23599
[38] Kazak M, Selin Koymen S, Yurdan R, Tekdemir K, Donmez N. Effect of thermal aging procedure on the microhardness and surface roughness of fluoride containing materials. Annals of Medical Research 2021;27:0888-94. https://doi.org/10.5455/annalsmedres.2019.12.831
[39] Gale M S, Darvell B W. Thermal cycling procedures for laboratory testing of dental restorations. J Dent 1999;27:89-99. https://doi.org/10.1016/S0300-5712(98)00037-2
[40] Pieniak D, Niewczas A, Walczak A, Łępicka M, Grądzka-Dahlke M, Maciejewski R, et al. The effect of thermal stresses on the functional properties of

various dental composites. Tribology International 2020;152:106509. https://doi.org/10.1016/j.triboint.2020.106509
[41] Druck C C, Pozzobon J L, Callegari G L, Dorneles L S, Valandro L F. Adhesion to Y-TZP ceramic: Study of silica nanofilm coating on the surface of Y-TZP. J Biomed Mater Res Part B 2015;103:143-50. https://doi.org/10.1002/jbm.b.33184
[42] Yan Y, Chen C, Chen B, Shen J, Zhang H, Xie H. Effects of hydrothermal aging, thermal cycling, and water storage on the mechanical properties of a machinable resin-based composite containing nano-zirconia fillers. J Mech Behav Biomed Mater 2020;102:103522. https://doi.org/10.1016/j.jmbbm.2019.103522
[43] Leyva del Rio D, Johnston W M. Effect of monomer composition and filler fraction on surface microhardness and depth of cure of experimental resin composites. Eur J Oral Sci 2023;131:e12933. https://doi.org/10.1111/eos.12933
[44] Pereni C I, Zhao Q, Liu Y, Abel E. Surface free energy effect on bacterial retention. Colloids and Surfaces B: Biointerfaces 2006;48:143-7. https://doi.org/10.1016/j.colsurfb.2006.02.004
[45] Hao Y, Huang X, Zhou X, Li M, Ren B, Peng X, et al. Influence of dental prosthesis and restorative materials interface on oral biofilms. Int J Mol Sci. 2018;19:3157. https://doi.org/10.3390/ijms19103157
[46] Kerby R E, Knobloch L A, Schricker S, Gregg B. Synthesis and evaluation of modified urethane dimethacrylate resins with reduced water sorption and solubility. Dent Mater 2009;25:302-13. https://doi.org/10.1016/j.dental.2008.07.009
[47] Procópio A L F, da Silva R A, Maciel J G, Sugio C Y C, Soares S, Urban V M, et al. Antimicrobial and cytotoxic effects of denture base acrylic resin impregnated with cleaning agents after long-term immersion. Toxicology in Vitro 2018;52:8-13. https://doi.org/10.1016/j.tiv.2018.05.012